Novel four-dimensional autonomous chaotic system generating one-, two-, three- and four-wing attractors

Yu Fei(余 飞), Wang Chun-Hua(王春华)†, Yin Jin-Wen(尹晋文), and Xu Hao(徐 浩)

College of Information Science and Engineering, Hunan University, Changsha 410082, *China*

(Received 27 May 2011; revised manuscript received 17 June 2011)

In this paper, we propose a novel four-dimensional autonomous chaotic system. Of particular interest is that this novel system can generate one-, two, three- and four-wing chaotic attractors with the variation of a single parameter, and the multi-wing type of the chaotic attractors can be displayed in all directions. The system is simple with a large positive Lyapunov exponent and can exhibit some interesting and complicated dynamical behaviours. Basic dynamical properties of the four-dimensional chaotic system, such as equilibrium points, the Poincaré map, the bifurcation diagram and the Lyapunov exponents are investigated by using either theoretical analysis or numerical method. Finally, a circuit is designed for the implementation of the multi-wing chaotic attractors. The electronic workbench observations are in good agreement with the numerical simulation results.

Keywords: multi-wing chaotic attractors, four-dimensional chaotic system, Poincaré map, bifurcation diagram

PACS: 05.45.Jn **DOI:** 10.1088/1674-1056/20/11/110505

1. Introduction

In recent decades, chaos has been intensively studied in many fields including engineering science, medical science and biology.[1−3] Since Lorenz found the first chaotic attractor during his study of the atmospheric convection in 1963,[4] many new chaotic attractors have been proposed, including the Rössler system,[5] the Chen system,[6] the Lü system,[7] the Liu system[8] and the generalized Lorenz system family.[9] As is well known, the chaotic dynamics of most Lorenz-like systems is confined in the positive half space with respect to the z axis or its mirror due to the limiting threshold effect,[10] which can generate only two-wing chaotic attractors, therefore, how to break such a threshold effect to generate multi-wing chaotic attractors in a simple autonomous system is worth studying.

There are several approaches to the break of such a threshold effect in a three-dimensional (3D) autonomous system. One is to make the z axis doubly polarized. Deng *et al.*[11] proposed a four-wing 3D chaotic system by making the z axis doubly polarized based on the Lü system. The second approach is to use the coupling theory. Grassi[12] and Grassi *et al.*[13] reported that four-wing (eight-wing) hyperchaotic attractors could be generated by coupling two (three) identical Lorenz systems. The third method is to use a piecewise-linear (PWL) function. Yu *et al.*[10] introduced a piecewise Lorenz system equipped with a staircase function and an even symmetric piecewise-linear function, which could generate various grid multi-wing butterfly chaotic attractors. The last one is to use a general method, where a smooth quadratic autonomous system is directly used. The system generally needs to satisfy some conditions,[14] i.e., (i) there is at least one quadratic term in each equation; (ii) the system has five equilibria; (iii) there is at least one linear term in each equation of the system. Qiao and Bao[15] proposed a four-wing 3D chaotic system, which verified the feasibility and validity of the above method. Chen *et al.*[16] presented a 3D smooth quadratic autonomous chaotic system, which could generate a single four-wing attractor and a single three-wing attractor. Dadras and Momeni[17] proposed a 3D autonomous chaotic system that could produce two-, three- and four-scroll chaotic attractors with the variation of a single parameter.

In order to construct a chaotic system with a more complicated topological structure, recently, four-wing four-dimensional (4D) chaotic systems were also proposed. Qi *et al.*[18] and Wang *et al.*[19] added a simple state feedback term to a 4D chaotic system. Although the chaotic system could display a fully qualified multi-wing type in all directions, it could generate only two- and four-wing chaotic attractors. And

†Corresponding author. E-mail: wch1227164@sina.com

© 2011 Chinese Physical Society and IOP Publishing Ltd

the circuit realization needed eight analog multipliers, since each equation of the system contained a cubic cross-product term. Dadras and Momeni[20] proposed a 4D chaotic system, which could generate one-, two-, three- and four-scroll chaotic attractors with appropriate choices of parameters, however the multi-scroll types of the system in some directions were less obvious. Therefore, it is very interesting to ask whether there exists a simple 4D autonomous system that can generate one-, two-, three- and four-wing attractors with the variation of a single parameter and can exhibit the multi-wing type in all directions simultaneously. This paper gives a positive answer to the above question by showing a new 4D autonomous system. The analyses of the bifurcation diagram and the Lyapunov exponents show that the new chaotic system has extremely complicated dynamical behaviours. Moreover, a module based circuit, which needs only three analog multipliers, is designed for the implementation. The electronic workbench (EWB) observations are used for the verification and demonstration.

2. Novel 4D chaotic system

Base on the general method,[14] we introduce a nonlinear state feedback controller u into the third equation, then a novel simple 4D autonomous chaotic system is expressed as

$$\begin{cases} \dot{x} = yz - ax, \\ \dot{y} = by - xz, \\ \dot{z} = xy - cz + du, \\ \dot{u} = xz - eu, \end{cases} \tag{1}$$

where a, b, c, d, e are system parameters, x, y, z are state variables, and u is the nonlinear state feedback controller. System (1) can generate one-, two-, three- and four-wing attractors with the variation of a single parameter. For example, system (1) with parameters of $a = 10$, $b = 12$, $c = 50$, $d = 2$, $e = 4$ and the initial condition of $[2, 1, 1, 2]^{\mathrm{T}}$ can generate new four-wing chaotic attractors. The four-wing attractors are displayed in Fig. 1. It appears that the new attractors exhibit interesting, complicated and abundant chaotic dynamical behaviours and there is a fully qualified four-wing type in all directions of the chaotic attractor. The Lyapunov exponents of system (1) are found to be $l_1 = 2.8836$, $l_2 = 0$, $l_3 = -3.4834$ and $l_4 = -50.2984$. It can be seen that there is a larger positive Lyapunov exponent.

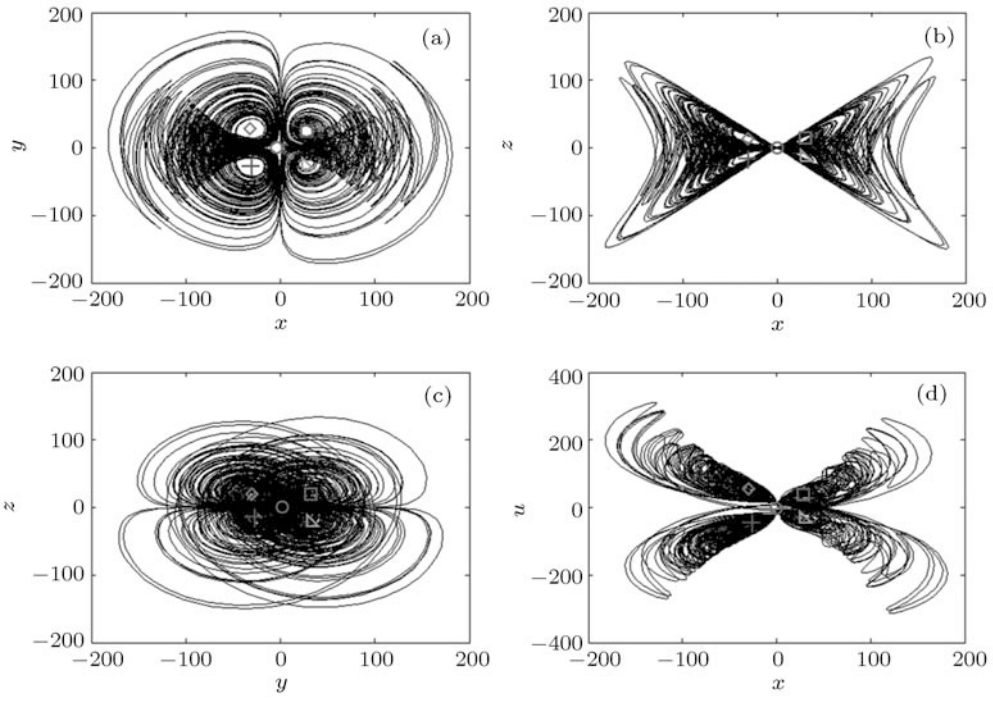


Fig. 1. Four-wing attractors of system (1) with $a = 10$, $b = 12$, $c = 50$, $d = 2$, and $e = 4$ in (a) x–y, (b) x–z, (c) y–z, and (d) x–u planes. Symbols ◯, □, +, △, and ♢ denote S_0, S_1, S_2, S_3 and S_4, respectively.

3. Dynamical behaviour of the novel 4D chaotic system

3.1. Four-wing chaotic attractor

It is obvious that the new system is not asymmetric with respect to any point or plane. Note that

$$\Delta V = \frac{\partial \dot{x}}{\partial x} + \frac{\partial \dot{y}}{\partial y} + \frac{\partial \dot{z}}{\partial z} + \frac{\partial \dot{u}}{\partial u} = -a + b - c - e,$$

so the system is dissipative as long as $-a+b-c-e < 0$, which means that a volume element V_0 is contracted by the flow into a volume element $V_0\,\mathrm{e}^{-a+b-c-e}$ at time t.

To analyse the system, a good start is to find its equilibria. It is clear that the origin is a trivial equilibrium of system (1). In order to obtain the non-zero equilibria, we consider the equilibrium of system (1) and let

$$\begin{cases} yz - ax = 0, \\ by - xz = 0, \\ xy - cz + du = 0, \\ xz - eu = 0. \end{cases} \tag{2}$$

If $a > 0$, $b > 0$ and $e \neq 0$, there are four nontrivial equilibria, which are described respectively as

$$S_{1,2} = \left(\sqrt{\frac{b}{a}} K_{1,2}, K_{1,2}, \sqrt{ab}, \frac{b}{e} K_{1,2} \right),$$
$$S_{3,4} = \left(\sqrt{\frac{b}{a}} K_{1,2}, -K_{1,2}, -\sqrt{ab}, -\frac{b}{e} K_{1,2} \right), \tag{3}$$

where

$$K_{1,2} = \frac{-(bd/e) \pm \sqrt{(b^2 d^2/e^2) + 4bc}}{2\sqrt{b/a}}. \tag{4}$$

when $a = 10$, $b = 12$, $c = 50$, $d = 2$ and $e = 4$, there are five equilibria in system (1), which are

$$S_0 = (0, 0, 0, 0),$$
$$S_{1,3} = (21.6779, \pm 19.7891, \pm 10.9545, \pm 59.3673),$$
$$S_{2,4} = (-27.6778, \mp 25.2663, \pm 10.9545, \mp 83.0335).$$

In order to investigate the stability of all the equilibria, we consider the Jacobian matrices corresponding to the equilibria and calculate their eigenvalues. The results are shown in Table 1. According to the eigenvalues, we know that the equilibria of systems (1) are all saddle focus nodes, which means that the five equilibria are all unstable.

In Fig. 1, symbols ◯, □, +, △ and ♢ denote S_0, S_1, S_2, S_3 and S_4, respectively. It is notable that there are many orbitals freely running around S_0, S_1, S_2, S_3 and S_4, which play an important role in forming the four-wing attractor, since they connect the upper and the lower attractors together. The four nontrivial equilibria, S_1, S_2, S_3, and S_4, are located in the centres of the four wings of the attractor, and origin S_0 is the centre of the whole chaotic attractor, as shown in Fig. 1.

Table 1. Eigenvalues of the Jacobin matrices for all the equilibria.

	S_0	$S_{1,3}$	$S_{2,4}$
λ_1	–10	–55.2154	–56.3362
λ_2	12	3.8877+18.0236i	3.9405+23.0592i
λ_3	–50	3.887 –18.0236i	3.9405–23.0592i
λ_4	–4	–4.5599	–3.5448

A basic and prominent property of the chaotic system is its seemingly erratic behaviour.[17] Figure 2 shows the time domain waveform. It can be seen that the time domain waveform has a non-cyclical characteristic and variables of all orbitals can freely move across the boundary to the opposite side. Figure 3 shows the spectrum map of system (1), which exhibits a continuous broadband feature.

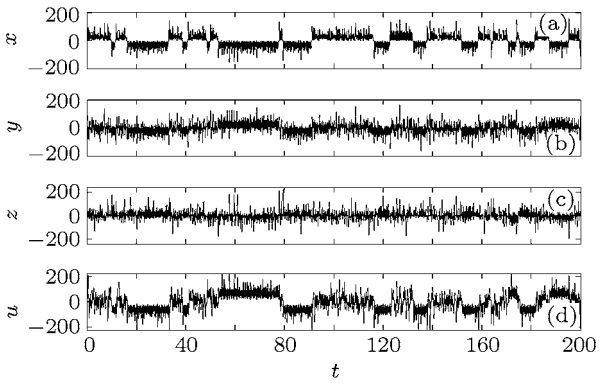


Fig. 2. Time domain waveforms of system (1) for (a) t–x, (b) t–y, (c) t–z, and (d) t–u waves.

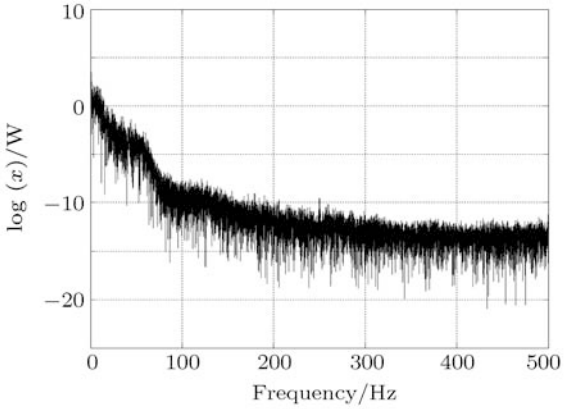


Fig. 3. Spectrum map of $\log|x|$.

3.2. Three-wing chaotic attractor

This new system can generate three-wing chaotic attractors by only varying a single parameter. Here, parameter c is selected to be varied. For example, if we choose $a = 10$, $b = 12$, $c = 60$, $d = 2$ and $e = 4$, three-wing chaotic attractors can be observed, as shown in Fig. 4. It can be seen that the system also has five equilibrium points. Further observation shows that the orbitals begin to move between two nontrivial equilibria and evolve into two-wing attractors on one side of the space. As time goes on, some orbitals begin to move the other nontrivial equilibria on the other side of the space and gradually form a three-wing chaotic attractor. The orbitals are always around the nontrivial equilibrium and do not escape. Therefore, the orbitals cannot freely run around the last nontrivial equilibrium and only generate three-wing chaotic attractors. The Lyapunov exponents of the system in this case are $l_1 = 1.6730$, $l_2 = 0$, $l_3 = -3.7227$ and $l_4 = -58.5859$. The third wing of the new chaotic attractor connects the other two wings. Hence, it has a more complicated topological structure than the classical two-wing Lorenz-like attractors.

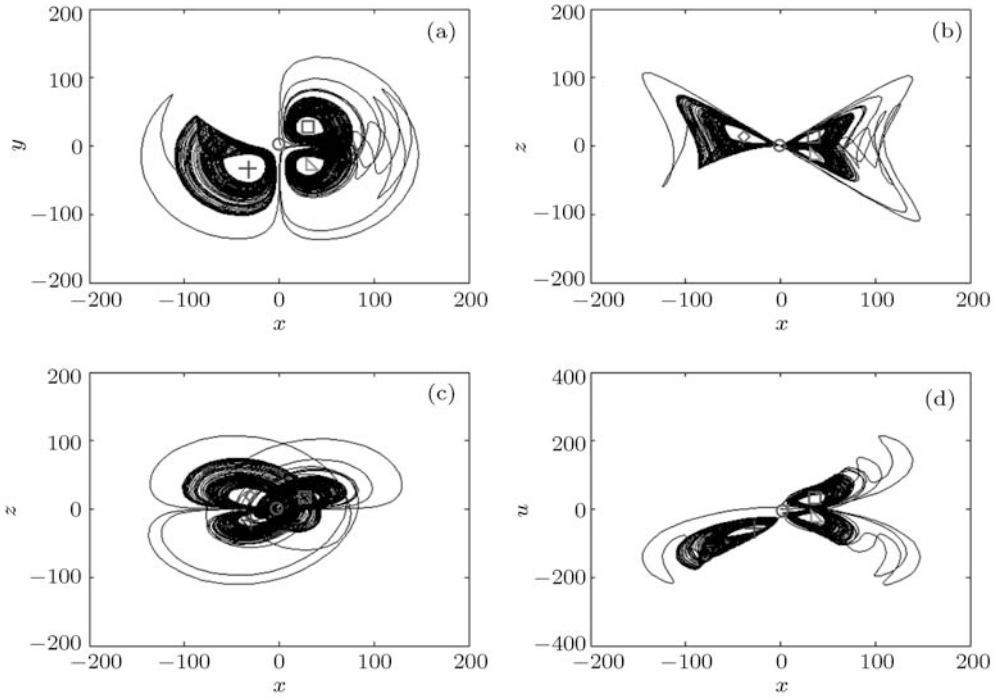


Fig. 4. Tree-wing attractors of system (1) with $a = 10$, $b = 12$, $c = 60$, $d = 2$ and $e = 4$ in (a) x–y, (b) x–z, (c) y–z, and (d) x–u planes.

3.3. Two-wing chaotic attractor

With parameters $a = 10$, $b = 12$, $c = 62$, $d = 2$ and $e = 4$, system (1) can also exhibit an attractor with two wings, as shown in Fig. 5. Making the same analysis as the above, we can show that the system also has five equilibrium points and the formation mechanism is similar to that of the three-wing chaotic attractor. The two-wing attractors can be called the upper and the lower attractors generated from the four-wing attractor. The Lyapunov exponents of the system in this case are found to be $l_1 = 1.0123$, $l_2 = 0$, $l_3 = -3.5669$ and $l_4 = -60.1261$.

3.4. One-wing chaotic attractor

Fixing parameters a, b, d and e, changing c, we can obtain a one-wing attractor. Here we choose $a = 10$, $b = 12$, $c = 53.5$, $d = 2$ and $e = 4$. With the above choice, the Lyapunov exponents of system (1) are $l_1 = 1.2971$, $l_2 = 0$, $l_3 = -3.4747$ and $l_4 = -52.1909$. It can be seen that the one-wing attractor is also a scroll, as shown in Fig. 6.

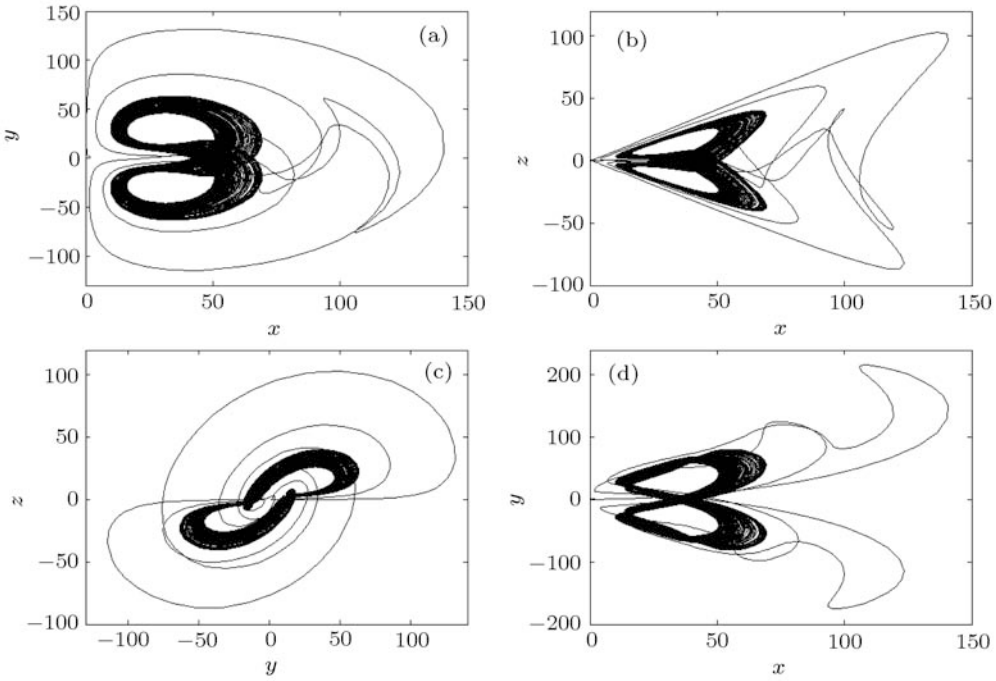


Fig. 5. Two-wing attractors of system (1) with $a = 10$, $b = 12$, $c = 62$, $d = 2$ and $e = 4$ in (a) x–y, (b) x–z, (c) y–z, and (d) x–u planes.

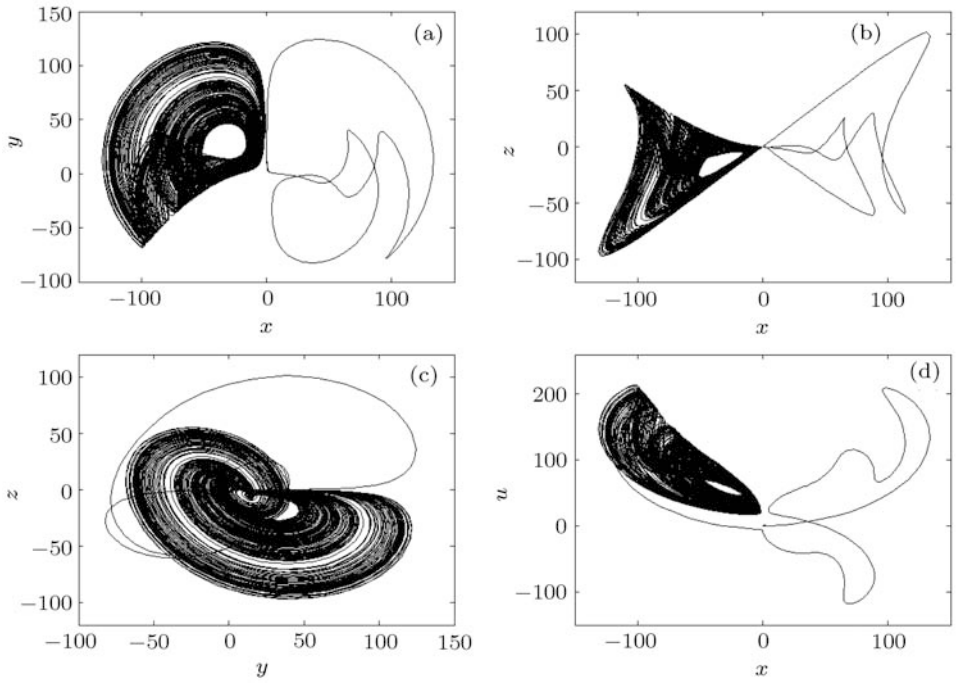


Fig. 6. One-wing attractors of system (1) with $a = 10$, $b = 12$, $c = 53.5$, $d = 2$ and $e = 4$ in (a) x–y, (b) x–z, (c) y–z, and (d) x–u planes.

4. Poincaré map, bifurcation diagram and Lyapunov exponent spectrum

The Poincaré map can reflect bifurcation and folding properties of chaos. The Poincaré map of system (1) projected on the x–y plane is shown in Fig. 7. It is clear that some sheets are folded, which indicates that the system has extremely rich dynamical behaviours. From the above analysis, it can be seen that parameter c is of essential importance, which determines the wing number of the new system. When we analyse parameter d, a very interesting phenomenon is found. The detail will be given below.

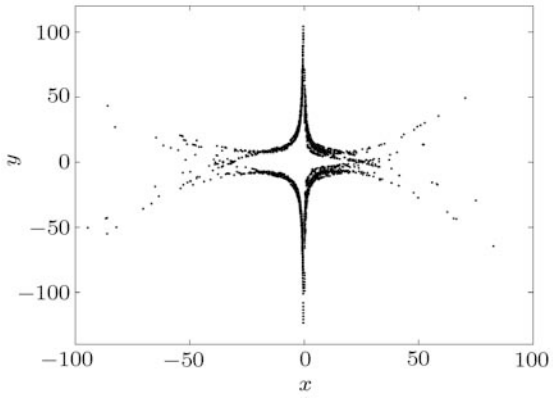


Fig. 7. Poincaré map of system (1) on the crossing section of $z = 0$.

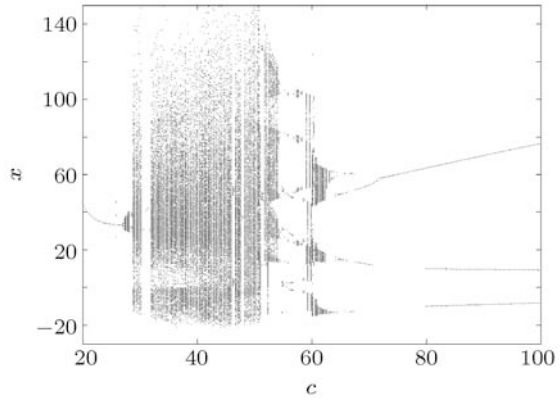


Fig. 8. Bifurcation diagram with the increasing c.

4.1. for fixed $a = 10$, $b = 12$, $d = 2$, $e = 4$ and varied c

Let c increase when other parameters are fixed. Figures 8 and 9 show the bifurcation diagram and the Lyapunov exponent spectrum varying with the increasing c. It can be seen that the bifurcation diagram well coincides with the spectrum of the Lyapunov exponent. When c increases, the system undergoes some representative dynamical routes, such as periodic orbitals, period-doubling bifurcation and chaos, which are summarized as follows. When $c \in [20, 24.5)$,

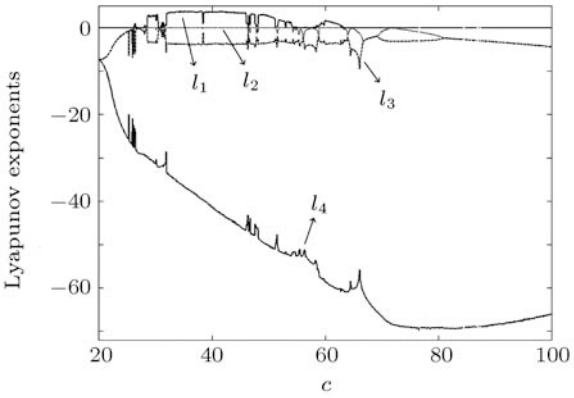


Fig. 9. Lyapunov exponent spectra with the increasing c.

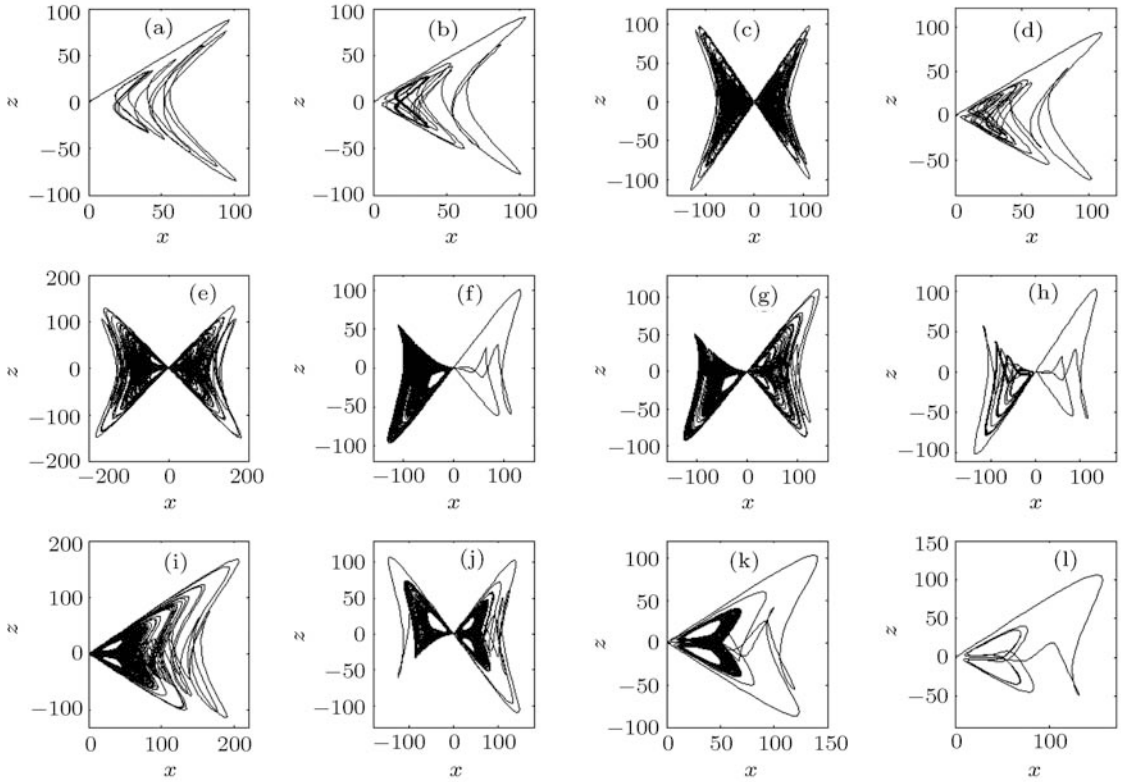


Fig. 10. Phase portraits in the x–z plane with different values of c: (a) $c = 22$, (b) $c = 27$, (c) $c = 29$, (d) $c = 37.3$, (e) $c = 50$, (f) $c = 53.5$, (g) $c = 54$, (h) $c = 57.5$, (i) $c = 59$, (j) $c = 60$, (k) $c = 60$, and (l) $c = 80$.

the system is in the periodic state (Fig. 10(a)); when $c \in [24.5, 28.1)$, the system has some quasi-periodic loops (Fig. 10(b)); when $c \in [28.1, 30.5)$, the system has the four-wing attractors (Fig. 10(c)); when $c \in [30.5, 31.9)$, the system has some quasi-periodic loops (Fig. 10(d)); when $c \in [31.9, 50.7)$, the system has the four-wing attractors (Fig. 10(e)); when $c \in [50.7, 54)$, the system has the one-wing attractor (Fig. 10(f)); when $c \in [54, 55.3)$, the system has the three-wing attractors (Fig. 10(g)); when $c \in [55.3, 58.5)$, the system undergoes the period-doubling bifurcation (Fig. 10(h)); when $c \in [58.5, 59.6)$, the system has the two-wing attractors (Fig. 10(i)); when $c \in [59.6, 60]$, the system has the three-wing attractors (Fig. 10(j)); when $c \in (60, 63.1)$, the system has the two-wing attractors (Fig. 10(k)); when $c \in [63.1, 100]$, the system undergoes the period-3 to period-2 and then to period-1 bifurcation, the periodic orbitals is shown in Fig. 10(l).

4.2. for fixed $a = 10$, $b = 12$, $c = 50$, $e = 4$ and varied d

Let d vary in the closed interval $[-20, 20]$, and other parameters are fixed. Figures 11 and 12 show the bifurcation diagram and the Lyapunov exponent spectrum versus d, respectively. It can be seen that the bifurcation diagram well coincides with the spectrum of the Lyapunov exponent. Besides, we also find they are symmetrical about $d = 0$ simultaneously.

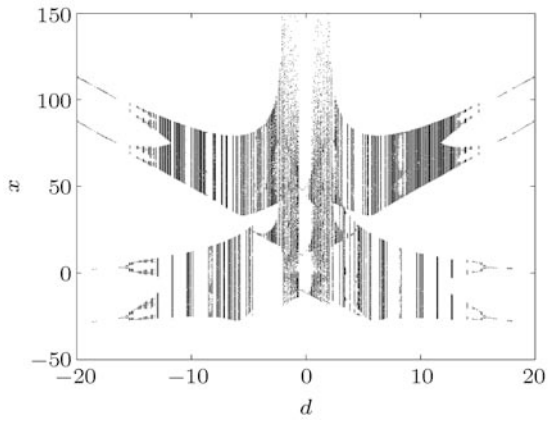


Fig. 11. Bifurcation diagram with the increasing d.

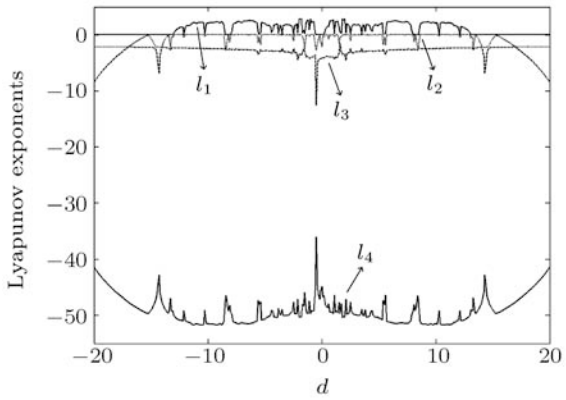


Fig. 12. Lyapunov exponents spectra with the increasing d.

5. Circuit implementation

In this section, the multi-wing 4D chaotic attractors are confirmed via a circuit design and EWB observations.

Figure 13 illustrates the electronic circuit diagram of the multi-wing chaotic attractors. The nonlinear terms in the equation are implemented with the analog multipliers AD633. Compared with the four-wing 4D chaotic attractors proposed in Refs [18] and [19], the new multi-wing 4D chaotic attractors just need three analog multipliers to be realized, while the chaotic attractors in Refs. [18] and [19] need eight analog multipliers to be realized. In the circuit, the value of resistor R_1, which mainly determines the wing number, is very important. When $R_1 = 2.243$ kΩ, the circuit generates the one-wing chaotic attractor (Fig. 14(a)); when $R_1 = 1.9355$ kΩ, the circuit creates the two-wing chaotic attractors (Fig. 14(b)); when $R_1 = 2$ kΩ, the circuit generates the three-wing chaotic attractors (Fig. 14(c)); when $R_1 = 2.4$ kΩ, the circuit generates the four-wing chaotic attractors (Fig. 14(d)). Here, R_1 should be a precision adjustable resistor.

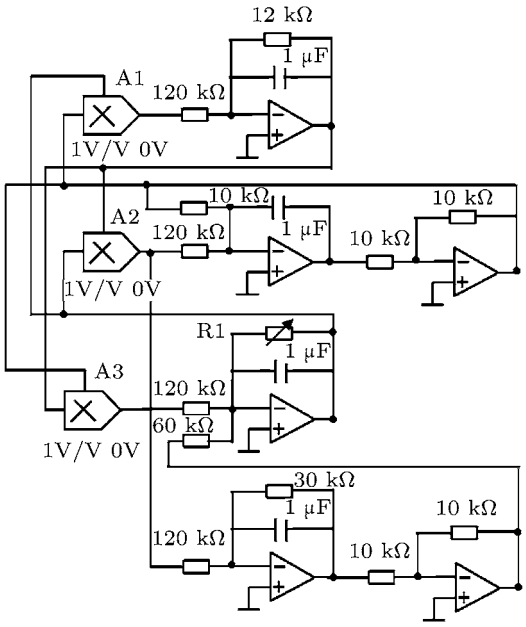


Fig. 13. Circuit implementation of system (1).

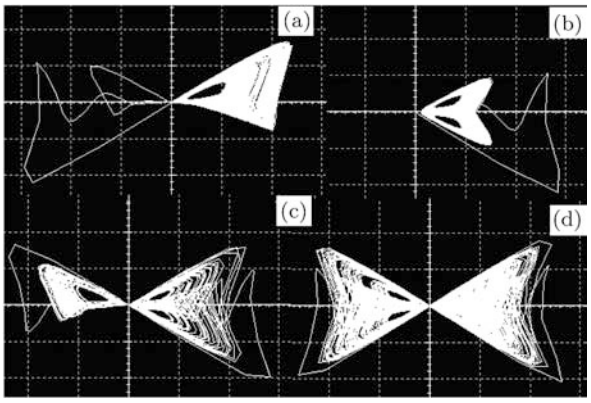


Fig. 14. EWB observations of the multi-wing attractors. (a) one-wing attractor, (b) two-wing attractors, (c) three-wing attractors, and (d) four-wing attractors.

6. Conclusion

In this paper, a new multi-wing 4D chaotic system is proposed and studied analytically and numerically. The new system can generate one-, two-, three- and four-wing chaotic attractors by varying a single parameter. Some basic dynamical behaviours of the system are studied. The analyses of the bifurcation diagram and the Lyapunov exponents show that the new chaotic system has extremely complicated dynamics. Finally, a circuit of the multi-wing chaotic attractors is designed and verified. Due to the fact that the switching mechanism between the multi-wing attractors is unknown,[20] the forming mechanism of the multi-wing system needs to be studied further in the future.

References

[1] Liu Z H, Zhang Y J, Zhang J and Wu J H 2011 *Acta Phys. Sin.* **60** 019501 (in Chinese)
[2] Di G H, Xu Y, Xu W and Gu R C 2011 *Acta Phys. Sin.* **60** 020504 (in Chinese)
[3] Han J J and Fu W J 2010 *Chin. Phys.* B **19** 010205
[4] Lorenz E N 1963 *J. Atmos. Sci.* **20** 130
[5] Rössler O E 1976 *Phys. Lett.* A **57** 397
[6] Chen G R and Ueta T 1999 *Int. J. Bifur. Chaos* **9** 1465
[7] Lü J H and Chen G R 2002 *Int. J. Bifur. Chaos* **12** 659
[8] Liu C, Liu T, Liu L and Liu K 2004 *Chaos Soliton. Fract.* **22** 1031
[9] Celikovsky S and Chen G R 2005 *Chaos Soliton. Fract.* **26** 1271
[10] Yu S M, Lü J H, Chen G R and Yu X H 2010 *IEEE Trans. Circuits Syst. II, Exp. Briefs.* **57** 803
[11] Deng B, Wang Z L, Hou C X and Yao F A 2010 *J. Univ. Jinan* (*Sci. and Tech.*) **24** 402 (in Chinese)
[12] Grassi G 2008 *Chin. Phys.* B **17** 3247
[13] Grassi G, Severance F L and Miller D A 2009 *Chaos Soliton. Fract.* **41** 284
[14] Wang Z, Qi G, Sun Y, van Wyk B J and van Wyk M A 2010 *Nonlinear Dyn.* **60** 443
[15] Qiao X H and Bao B C 2009 *Acta Phys. Sin.* **58** 8152 (in Chinese)
[16] Chen Z, Yang Y and Yuan Z 2008 *Chaos Soliton. Fract.* **38** 1187
[17] Dadras S and Momeni H R 2009 *Phys. Lett.* A **373** 3637
[18] Qi G Y, Chen G R and Zhang Y H 2008 *Chaos Soliton. Fract.* **37** 409
[19] Wang F Z, Qi G Y, Chen Z Q and Yuan Z Z 2007 *Acta Phys. Sin.* **56** 3137(in Chinese)
[20] Dadras S and Momeni H R 2010 *Chin. Phys.* B **19** 060506